









TECH BRIEFS

NATIONAL AERONAUTICS AND SPACE ADMINISTRATION

-  **Technology Focus**
-  **Computers/Electronics**
-  **Software**
-  **Materials**
-  **Mechanics**
-  **Machinery/Automation**
-  **Manufacturing**
-  **Bio-Medical**
-  **Physical Sciences**
-  **Information Sciences**
-  **Books and Reports**

INTRODUCTION

Tech Briefs are short announcements of innovations originating from research and development activities of the National Aeronautics and Space Administration. They emphasize information considered likely to be transferable across industrial, regional, or disciplinary lines and are issued to encourage commercial application.

Availability of NASA Tech Briefs and TSPs

Requests for individual Tech Briefs or for Technical Support Packages (TSPs) announced herein should be addressed to

National Technology Transfer Center

Telephone No. (800) 678-6882 or via World Wide Web at www2.nttc.edu/leads/

Please reference the control numbers appearing at the end of each Tech Brief. Information on NASA's Commercial Technology Team, its documents, and services is also available at the same facility or on the World Wide Web at www.nctn.hq.nasa.gov.

Commercial Technology Offices and Patent Counsels are located at NASA field centers to provide technology-transfer access to industrial users. Inquiries can be made by contacting NASA field centers and program offices listed below.

NASA Field Centers and Program Offices

Ames Research Center

Carolina Blake
(650) 604-1754
cblake@mail.arc.nasa.gov

Dryden Flight Research Center

Jenny Baer-Riedhart
(661) 276-3689
jenny.baer-riedhart@dfrc.nasa.gov

Goddard Space Flight Center

Nona Cheeks
(301) 286-5810
Nona.K.Cheeks.1@gssc.nasa.gov

Jet Propulsion Laboratory

Art Murphy, Jr.
(818) 354-3480
arthur.j.murphy-jr@jpl.nasa.gov

Johnson Space Center

Charlene E. Gilbert
(281) 483-3809
commercialization@jsc.nasa.gov

Kennedy Space Center

Jim Aliberti
(321) 867-6224
Jim.Aliberti-1@ksc.nasa.gov

Langley Research Center

Sam Morello
(757) 864-6005
s.a.morello@larc.nasa.gov

John H. Glenn Research Center at Lewis Field

Larry Viterna
(216) 433-3484
cto@grc.nasa.gov

Marshall Space Flight Center

Vernotto McMillan
(256) 544-2615
vernotto.mcmillan@msfc.nasa.gov

Stennis Space Center

Robert Bruce
(228) 688-1929
robert.c.bruce@nasa.gov

NASA Program Offices

At NASA Headquarters there are seven major program offices that develop and oversee technology projects of potential interest to industry:

Carl Ray

Small Business Innovation Research Program (SBIR) & Small Business Technology Transfer Program (STTR)
(202) 358-4652 or
cray@mail.hq.nasa.gov

Dr. Robert Norwood

Office of Commercial Technology (Code RW)
(202) 358-2320 or
rnorwood@mail.hq.nasa.gov

John Mankins

Office of Space Flight (Code MP)
(202) 358-4659 or
jmankins@mail.hq.nasa.gov

Terry Hertz

Office of Aero-Space Technology (Code RS)
(202) 358-4636 or
thertz@mail.hq.nasa.gov

Glen Mucklow

Office of Space Sciences (Code SM)
(202) 358-2235 or
gmucklow@mail.hq.nasa.gov

Roger Crouch

Office of Microgravity Science Applications (Code U)
(202) 358-0689 or
rcrouch@hq.nasa.gov

Granville Paules

Office of Mission to Planet Earth (Code Y)
(202) 358-0706 or
gpaules@mtpe.hq.nasa.gov



TECH BRIEFS

NATIONAL AERONAUTICS AND SPACE ADMINISTRATION



5 Technology Focus: Sensors

- 5 Using Diffusion Bonding in Making Piezoelectric Actuators
- 6 Wireless Temperature-Monitoring System
- 7 Analog Binaural Circuits for Detecting and Locating Leaks
- 7 Mirrors Containing Biomimetic Shape-Control Actuators



9 Computers/Electronics

- 9 Surface-Micromachined Planar Arrays of Thermopiles
- 10 Cascade Back-Propagation Learning in Neural Networks



13 Materials

- 13 Perovskite Superlattices as Tunable Microwave Devices
- 14 Rollable Thin-Shell Nanolaminate Mirrors



15 Mechanics

- 15 Flight Tests of a Ministick Controller in an F/A-18 Airplane
- 16 Piezoelectrically Actuated Shutter for High Vacuum



17 Machinery/Automation

- 17 Bio-Inspired Engineering of Exploration Systems



19 Manufacturing

- 19 Microscope Cells Containing Multiple Micromachined Wells
- 20 Electrophoretic Deposition for Fabricating Microbatteries



21 Physical Sciences

- 21 Integrated Arrays of Ion-Sensitive Electrodes
- 22 Model of Fluidized Bed Containing Reacting Solids and Gases
- 23 Membrane Mirrors With Bimorph Shape Actuators



25 Information Sciences

- 25 Using Fractional Clock-Period Delays in Telemetry Arraying
- 26 Developing Generic Software for Spacecraft Avionics



27 Books & Reports

- 27 Numerical Study of Pyrolysis of Biomass in Fluidized Beds
- 27 Assessment of Models of Chemically Reacting Granular Flows

This document was prepared under the sponsorship of the National Aeronautics and Space Administration. Neither the United States Government nor any person acting on behalf of the United States Government assumes any liability resulting from the use of the information contained in this document, or warrants that such use will be free from privately owned rights.



Using Diffusion Bonding in Making Piezoelectric Actuators

Fabrication is simplified and performance improved.

Lyndon B. Johnson Space Center, Houston, Texas

A technique for the fabrication of piezoelectric actuators that generate acceptably large forces and deflections at relatively low applied voltages involves the stacking and diffusion bonding of multiple thin piezoelectric layers coated with film electrodes. The present technique stands in contrast to an older technique in which the layers are bonded chemically, by use of urethane or epoxy agents.

The older chemical-bonding technique entails several disadvantages, including the following:

- It is difficult to apply the bonding agents to the piezoelectric layers.
- It is difficult to position the layers accurately and without making mistakes.
- There is a problem of disposal of hazardous urethane and epoxy wastes.
- The urethane and epoxy agents are nonpiezoelectric materials. As such, they contribute to the thickness of a

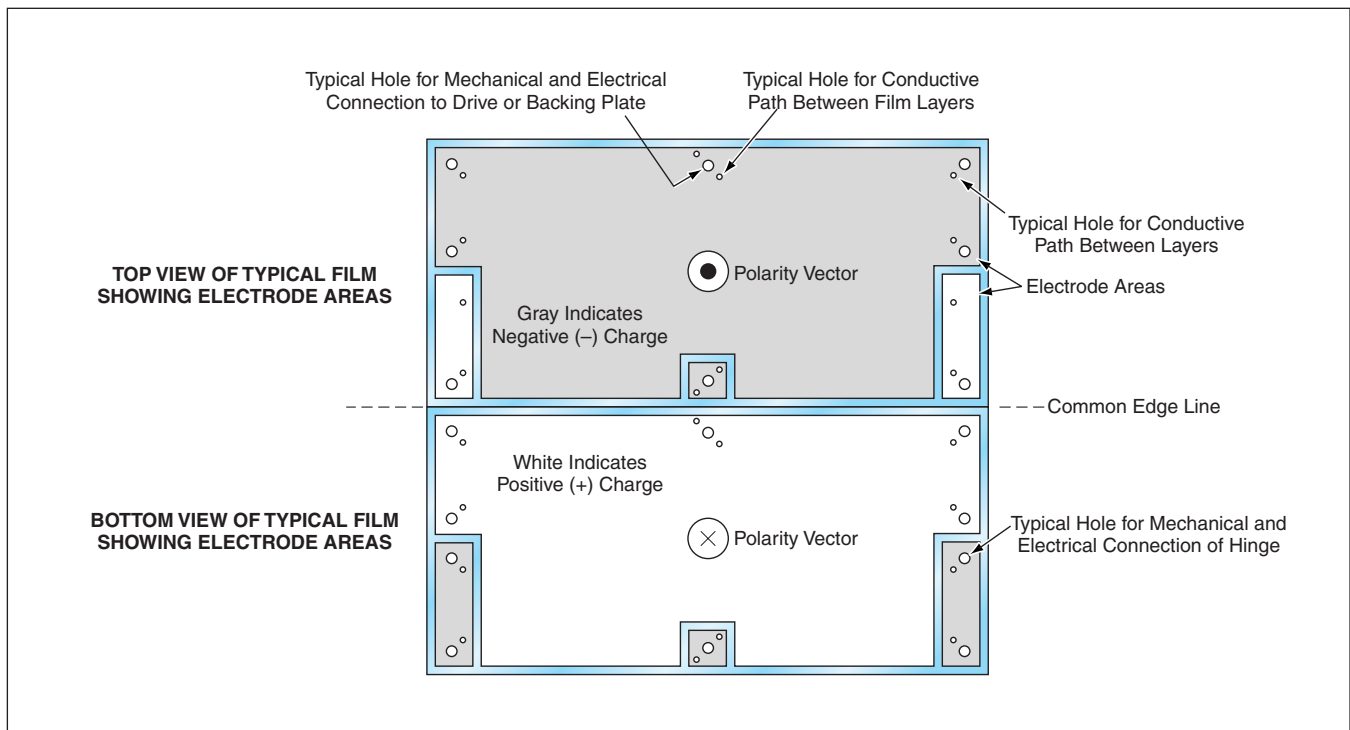
piezoelectric laminate without contributing to its performance; conversely, for a given total thickness, the performance of the laminate is below that of a unitary piezoelectric plate of the same thickness.

The figure depicts some aspects of the fabrication of a laminated piezoelectric actuator by the present diffusion-bonding technique. First, stock sheets of the piezoelectric material are inspected and tested. Next, the hole pattern shown in the figure is punched into the sheets. Alternatively, if the piezoelectric material is not a polymer, then the holes are punched in thermoplastic films. Then both faces of each punched piezoelectric sheet or thermoplastic film are coated with a silver-ink electrode material by use of a silk-screen printer. The electrode and hole patterns are designed for minimal complexity and minimal waste of material.

After a final electrical test, all the coated piezoelectric layers (or piezoelectric layers and coated thermoplastic films) are stacked in an alignment jig, which, in turn, is placed in a curved press for the diffusion-bonding process. In this process, the stack is pressed and heated at a specified curing temperature and pressure for a specified curing time. The pressure, temperature, and time depend on the piezoelectric material selected. At the end of the diffusion-bonding process, the resulting laminated piezoelectric actuator is tested to verify the adequacy of the mechanical output as a function of an applied DC voltage.

The principal advantages of the diffusion-bonding process over the older chemical-bonding process are the following:

- No adhesive thinner or hardening agent is needed;
- There are no waste chemicals;



The **Layout of Holes and Electrode Areas** on a piezoelectric layer provides for mechanical and electrical connections among stacked identical layers. The shading of electrode areas shows a typical state of charge encountered during operation. Although one layer is shown here, a prototype containing 40 such layers has been fabricated.

- Cure can be done at a relatively low temperature;
- There is less handling of piezoelectric sheets;
- No special adhesive-handling equipment is needed;
- The thickness contributed by the thermoplastic adhesive material (if used) is minimal;
- Diffusion bonding results in high-strength bonds that impart high durability and long fatigue life.
- In the case of polymeric piezoelectric layers, piezoelectric properties are improved, probably because of an increase in Young's modulus associated

with annealing during diffusion bonding.

- There is a significant reduction in electrical wiring: The electrode and hole patterns in the stacked layers give rise to an internal topology equivalent to that of a continuously folded length of piezoelectric material. As a result, the multiple electrical connections to the active piezoelectric layers are reduced to two terminal holes.

This work was done by Frank E. Sager of Oceaneering Space Systems for Johnson Space Center. Further information is contained in a TSP (see page 1).

Title to this invention, covered by U.S. Patent No. 5,761,782 has been waived under the provisions of the National Aeronautics and Space Act (42 U.S.C. 2457 (f)). Inquiries concerning licenses for its commercial development should be addressed to

*Mr. Jeff Brown
Oceaneering Space Systems
16665 Space Center Blvd.
Houston, TX 77598
Tel. No: (281) 488-9080 Ext. 3437
Fax No: (281) 488-6485*

Refer to MSC-22886, volume and number of this NASA Tech Briefs issue, and the page number.

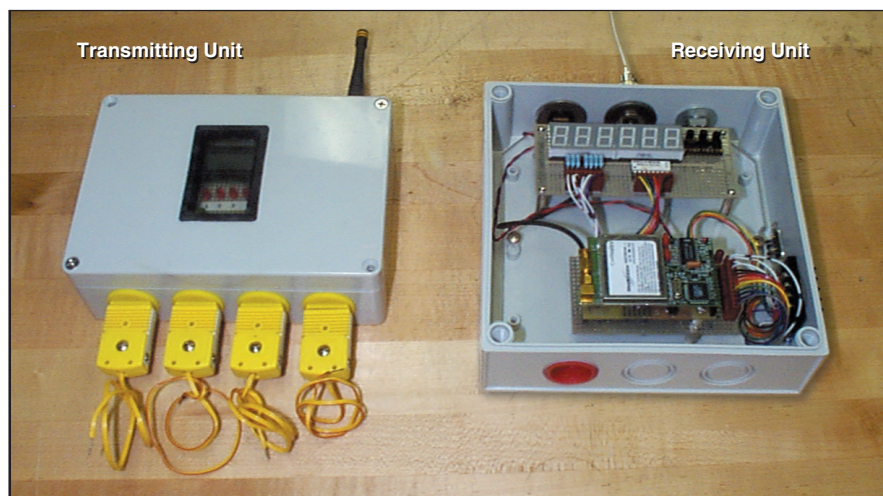
Wireless Temperature-Monitoring System

Sensors can be placed almost anywhere within 0.8 km of a receiving unit.

Stennis Space Center, Mississippi

A relatively inexpensive instrumentation system that includes units that are connected to thermocouples and that are parts of a radio-communication network has been developed to enable monitoring of temperatures at multiple locations. Because there is no need to string wires or cables for communication, the system is well suited for monitoring temperatures at remote locations and for applications in which frequent changes of monitored or monitoring locations are needed. The system can also be adapted to monitoring of slowly varying physical quantities, other than temperature, that can be transduced by solid-state electronic sensors.

The system comprises any number of transmitting units and a single receiving unit (see figure). Each transmitting unit includes connections for as many as four external thermocouples, a signal-conditioning module, a control module, and a radio-communication module. The signal-conditioning module acts as an interface between the thermocouples and the rest of the transmitting unit and includes a built-in solid ambient-temperature sensor that is in addition to the external thermocouples. The control module is a "system-on-chip" embedded processor that includes analog-to-digital converters, serial and parallel data ports, and an interface for local connection to an analog meter that is used during installation to verify correct operation. The radio-communication module contains a commercial spread-spectrum



A Transmitting Unit (One of Several) and the Receiving Unit communicate by spread-spectrum modulation at a carrier frequency near 900 MHz. The use of spread-spectrum modulation minimizes interference to other radio-communication systems.

transceiver that operates in the 900-MHz industrial, scientific, and medical (ISM) frequency band. This transceiver transmits data to the receiving unit at a rate of 19,200 baud.

The receiving unit includes a transceiver like that of a transmitting unit, plus a control module that contains a system-on-chip processor that includes serial data port for output to a computer that runs monitoring and/or control software, a parallel data port for output to a printer, and a seven-segment light-emitting-diode display.

Each transmitting unit is battery-powered and can operate for at least seven days continuously while reporting temperatures every half hour. The receiving

unit is powered by a wall-mounted transformer source. The receiving unit responds to each transmitting unit and reports the readings of each of the four thermocouples and of the ambient-temperature sensor of the transmitting unit. The end-to-end accuracy of the system is ± 0.2 °C over the temperature range from 0 to 100 °C. The radio-communication range between the receiving and transmitting units is ≈ 0.5 mile (≈ 0.8 km).

This work was done by Wanda Solano and Chuck Thurman of Stennis Space Center.

Inquiries concerning rights for the commercial use of this invention should be addressed to the Intellectual Property Manager, Stennis Space Center; (228) 688-1929. Refer to SSC-00163.

Analog Binaural Circuits for Detecting and Locating Leaks

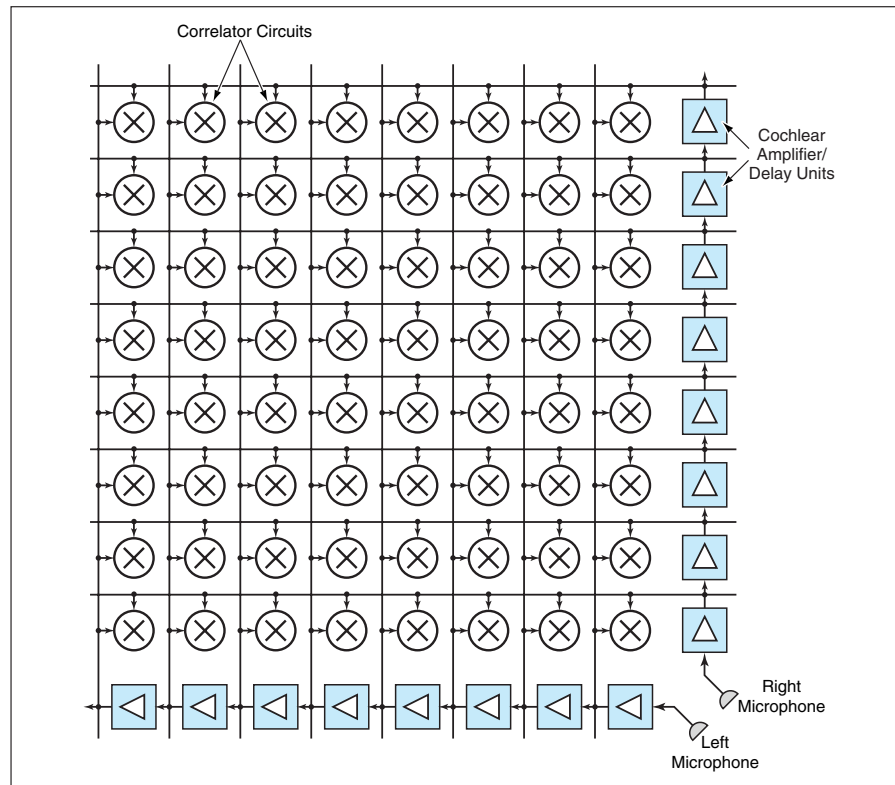
Ultrasonic signals received by paired transducers would be correlated to measure differential delays.

NASA's Jet Propulsion Laboratory, Pasadena, California

Very-large-scale integrated (VLSI) analog binaural signal-processing circuits have been proposed for use in detecting and locating leaks that emit noise in the ultrasonic frequency range. These circuits would be designed to function even in the presence of intense lower-frequency background noise that could include sounds associated with flow and pumping. Each of the proposed circuits would include the approximate electronic equivalent of a right and a left cochlea plus correlator circuits.

A pair of transducers (microphones or accelerometers), corresponding to right and left ears, would provide the inputs to their respective cochleas from different locations (e.g., from different positions along a pipe). The correlation circuits plus some additional external circuits would determine the difference between the times of arrival of a common leak sound at the two transducers. Then the distance along the pipe from either transducer to the leak could be estimated from the time difference and the speed of sound along the pipe. If three or more pairs of transducers and cochlear/correlator circuits were available and could suitably be positioned, it should be possible to locate a leak in three dimensions by use of sound propagating through air.

The cochlear circuits would consist mostly of cascades of amplifier/delay units positioned along two orthogonal edges of a rectangular VLSI chip, as depicted in the figure in simplified form. In addition to introducing increments of delay, the cochlear circuits would filter the signals to reject frequencies below the ultrasonic range. The output of a given amplifier/delay unit in a cochlea would



Cochlear and Correlator Circuits, operating in conjunction with external scanning circuits, would implement stereausis.

be fed to both the next amplifier/delay unit in the same cochlea and to a string of correlator circuits, which would form the analogs of the correlations between (1) the output of this unit and (2) the outputs of all amplifier/delay units in the other cochlea. The outputs of the correlator circuits would be scanned by the external circuitry and displayed or otherwise processed to determine which pairings of right and left cochlear units (and thus which differential signal

delay) yields the greatest correlations.

This work was done by Frank T. Hartley of Caltech for NASA's Jet Propulsion Laboratory. Further information is contained in a TSP (see page 1).

This invention is owned by NASA, and a patent application has been filed. Inquiries concerning nonexclusive or exclusive license for its commercial development should be addressed to the Patent Counsel, NASA Management Office-JPL; (818) 354-7770. Refer to NPO-18399.

Mirrors Containing Biomimetic Shape-Control Actuators

Local bending would be controlled to obtain desired surface figures.

NASA's Jet Propulsion Laboratory, Pasadena, California

Curved mirrors of a proposed type would comprise lightweight sheets or films containing integral, biologically inspired actuators for controlling their surface figures. These mirrors could be useful in such applications as collection

of solar energy, focusing of radio beams, and (provided sufficient precision could be achieved) imaging. These mirrors were originally intended for use in outer space, but it should also be possible to develop terrestrial versions.

Several prior NASA Tech Briefs articles have described a variety of approaches to the design of curved, lightweight mirrors containing integral shape-control actuators. The primary distinction between the present approach and the prior ap-

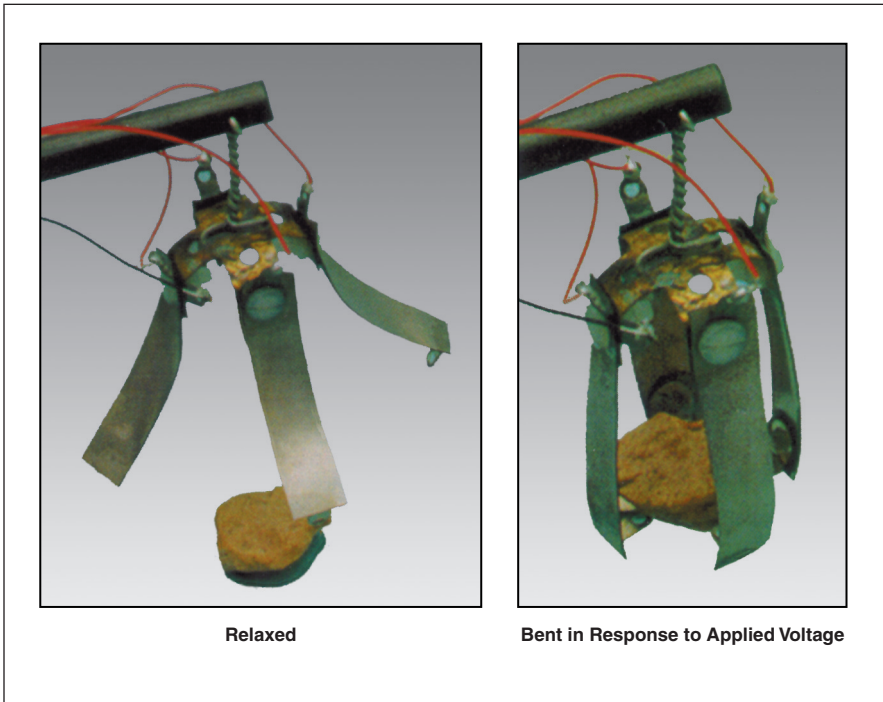


Figure 1. IPMC Multifinger Grippers have been adopted as models from which designs of proposed shape-controllable mirrors would be developed.

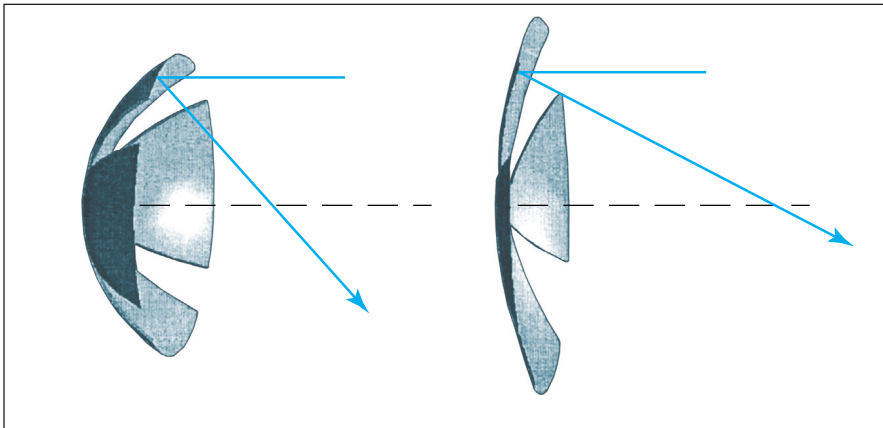


Figure 2. The Focal Length of a Curved Mirror would be varied by using its shape actuators to vary its curvature.

proaches lies in the actuator design concept, which involves shapes and movements reminiscent of those of a variety of small, multi-armed animals. The shape and movement of an actuator of this type can also be characterized as reminiscent of that of an umbrella. This concept can be further characterized as a derivative of that of multifinger grippers, the fingers of which are bimorph bending actuators (see Figure 1). The fingers of such actuators can be strips containing any of a variety of materials that have been investigated for use as actuators, including such electroactive polymers as ionomeric polymer/metal composites (IPMCs), ferroelectric polymers, and grafted elastomers.

A mirror according to this proposal would be made from a sheet of one of the actuator composites mentioned above. The design would involve many variables, including the pre-curvature and stiffness of the mirror sheet, the required precision of figure control, the required range of variation in focal length (see Figure 2), the required precision of figure control for imaging or non-imaging use, the bending and twisting moments needed to effect the required deformations, and voltage-to-moment coefficients of the actuators, and the voltages accordingly required for actuation. A typical design would call for segmentation of the electrodes on the actuators so that voltages could be applied locally to effect local bending for fine adjustment of the surface figure.

This work was done by Yoseph Bar-Cohen, Pantazis Mouroulis, Xiaoqi Bao, and Stewart Sherrit of Caltech for NASA's Jet Propulsion Laboratory. Further information is contained in a TSP (see page 1). NPO-30487



Surface-Micromachined Planar Arrays of Thermopiles

Several design features are expected to afford improved performance.

NASA's Jet Propulsion Laboratory, Pasadena, California

Planar two-dimensional arrays of thermopiles intended for use as thermal-imaging detectors are to be fabricated by a process that includes surface micromachining. These thermopile arrays are designed to perform better than do prior two-dimensional thermopile arrays.

The lower performance of prior two-dimensional thermopile arrays is attributed to the following causes:

- The thermopiles are made from low-performance thermoelectric materials.
- The devices contain dielectric supporting structures, the thermal conductances of which give rise to parasitic losses of heat from detectors to substrates.
- The bulk-micromachining processes sometimes used to remove substrate material under the pixels, making it difficult to incorporate low-noise readout electronic circuitry.
- The thermoelectric lines are on the same level as the infrared absorbers, thereby reducing fill factor.

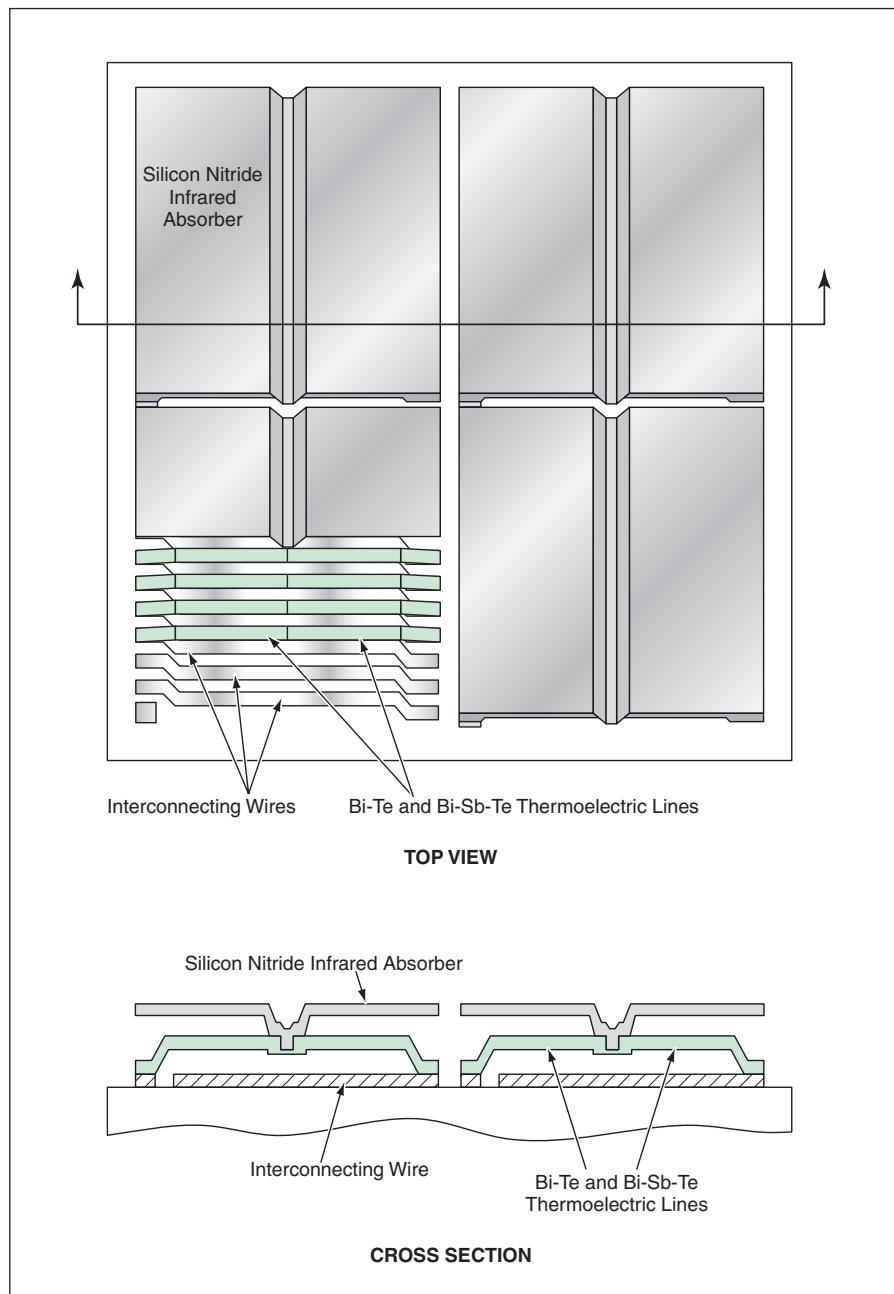
The improved pixel design of a thermopile array of the type under development is expected to afford enhanced performance by virtue of the following combination of features:

- Surface-micromachined detectors are thermally isolated through suspension above readout circuitry.
- The thermopiles are made of such high-performance thermoelectric materials as Bi-Te and Bi-Sb-Te alloys.
- Pixel structures are supported only by the thermoelectric materials: there are no supporting dielectric structures that could leak heat by conduction to the substrate.
- To maximize response, there are many thin thermoelectric legs only about 2 μm wide.
- The thermoelectric legs are hidden under a silicon nitride infrared-absorbing structure, making a large fill factor for the absorber.

The figure depicts selected aspects of four-pixel example of the improved design. The device can be characterized as a three-layer structure (or a four-layer structure if one includes the substrate).

During fabrication, the device also contains two sacrificial layers, typically composed of polyimide. One sacrificial layer

is located over interconnecting wires and under the thermoelectric lines; the other sacrificial layer is located over the ther-



The **Removal of Sacrificial Layers** during fabrication thermally isolates the absorber, reducing heat leaks and thereby increasing responsivity. The thinness of the thermoelectric lines and absorber makes response time short.

moelectric lines and under the silicon nitride infrared absorber. After the detector structure is fabricated, the sacrificial layers are removed, typically by etching in an oxygen plasma. The removal of the sacrificial layers is what provides the thermal isolation mentioned above.

The design facilitates maximization of the number of thermoelectric legs to increase the responsivity and the electrical impedance of the detector. Using 2- μm widths and 2- μm spacings of thermoelectric lines, it is possible to place about 11 thermocouples under a 50- μm -wide pixel.

Absorption of infrared radiation is enhanced by use of a quarter-wave cavity. In

each pixel, a thin layer of metal on the silicon nitride layer constitutes a front absorber, while the thermoelectric legs and interconnecting wires, together, constitute a back-side mirror.

At the time of reporting the information for this article, partially completed detectors (lacking the silicon nitride absorbers) of 100- μm pixel size had been built and tested. The results of the test indicate a pixel resistance of 250 k Ω , responsivity of 1.5 kV/W, response time of 1.7 ms, and detectivity (D^*) of $2.4 \times 10^8 \text{ cm}\cdot\text{Hz}^{1/2}/\text{W}$. Improvements are ongoing.

This work was done by Marc C. Foote of

Caltech for NASA's Jet Propulsion Laboratory. Further information is contained in a TSP (see page 1).

In accordance with Public Law 96-517, the contractor has elected to retain title to this invention. Inquiries concerning rights for its commercial use should be addressed to

Intellectual Property group

JPL

Mail Stop 202-233

4800 Oak Grove Drive

Pasadena, CA 91109

(818) 354-2240

Refer to NPO-30124, volume and number of this NASA Tech Briefs issue, and the page number.

Cascade Back-Propagation Learning in Neural Networks

This method would be implemented in VLSI circuitry.

NASA's Jet Propulsion Laboratory, Pasadena, California

The cascade back-propagation (CBP) algorithm is the basis of a conceptual design for accelerating learning in artificial neural networks. The neural networks would be implemented as analog very-large-scale integrated (VLSI) circuits, and circuits to implement the CBP algorithm would be fabricated on the same VLSI circuit chips with the neural networks. Heretofore, artificial neural networks have learned slowly because it has been necessary to train them via software, for lack of a good on-chip learning technique. The CBP algorithm is an on-chip technique that provides for continuous learning in real time.

Artificial neural networks are trained by example: A network is presented with training inputs for which the correct outputs are known, and the algorithm strives to adjust the weights of synaptic connections in the network to make the actual outputs approach the correct outputs. The input data are generally divided into three parts. Two of the parts, called the "training" and "cross-validation" sets, respectively, must be such that the corresponding input/output pairs are known. During training, the cross-validation set enables verification of the status of the input-to-output transformation learned by the network to avoid overlearning. The third part of the data, termed the "test" set, consists of the inputs that are required to be transformed into outputs; this set may or may not include the training set and/or the cross-validation set.

Proposed neural-network circuitry for on-chip learning would be divided into two distinct networks; one for training and one for validation. Both networks would share the same synaptic weights. During training iterations, these weights would be continuously modulated according to the CBP algorithm, which is

so named because it combines features of the back-propagation and cascade-correlation algorithms. Like other algorithms for learning in artificial neural networks, the CBP algorithm specifies an iterative process for adjusting the weights of synaptic connections by descent along the gradient of an error measure in the

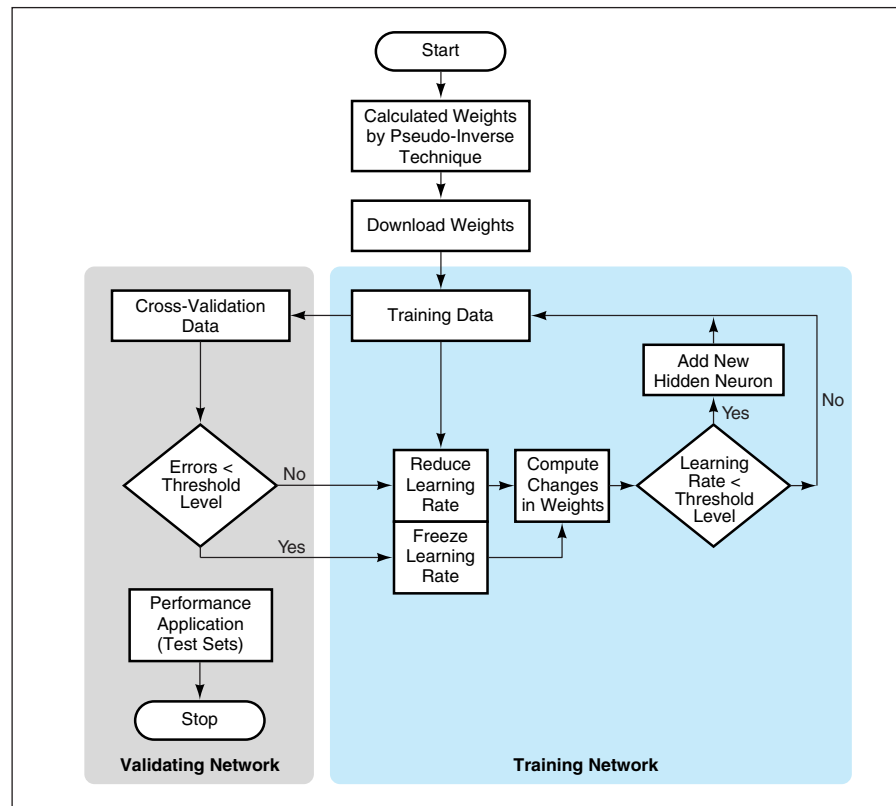


Figure 1. The Cascade Back-Propagation Algorithm provides the theoretical basis for design of an analog neural network that learns rapidly.

vector space of synaptic-connection weights. The error measure is usually a quadratic function of the differences between the actual and the correct outputs.

The CBP algorithm (see Figure 1) begins with calculation of the weights between the input and output layers of neurons by use of a pseudo-inverse technique. Then learning proceeds by gradient descent with the existing neurons as long as the rate of learning remains above a specified threshold level. When the rate of learning falls below this level, a new hidden neuron is added. When the quadratic error measure has descended to a value based on a predetermined criterion, the rate of learning is frozen. Thereafter, the network keeps learning endlessly with the existing neurons.

Figure 2 illustrates the cascade aspect of the CBP algorithm. To each newly added hidden neuron there are not only weighted connections from all the inputs but also a new dimension of inputs from the previous hidden neurons. The cascade aspect provides two important benefits: (1) it enables the network to get out of local minima of the quadratic error measure and (2) it accelerates convergence by eliminating the waste of time that would occur if gradient descent were allowed to occur in many equivalent subspaces of synaptic-connection-weight space. The cascade scheme concentrates learning

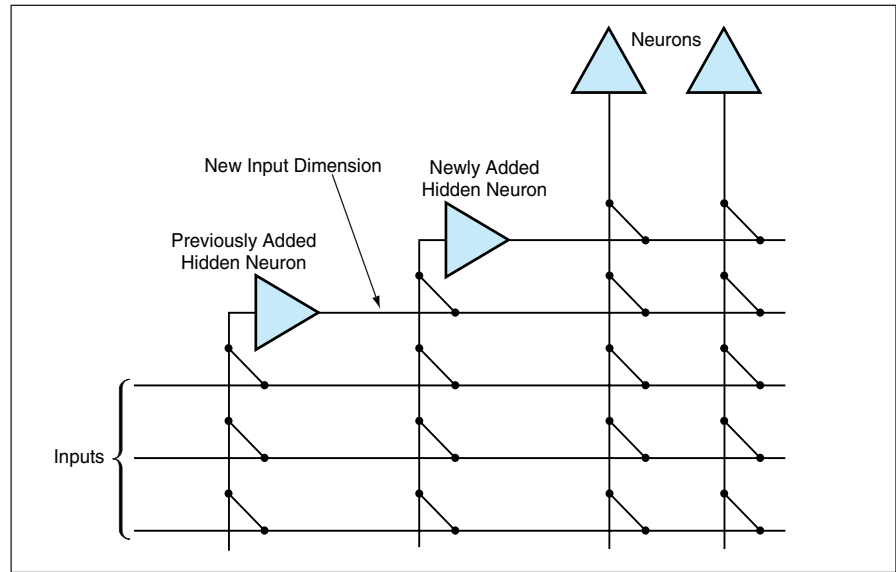


Figure 2. The **Cascade Configuration** of connections to added hidden neurons helps to accelerate convergence on the desired state of learning.

into one subspace that is a cone of a hypercube.

The gradient descent involves, among other things, computation of derivatives of neuron transfer curves. The proposed analog implementation would provide the effectively high resolution that is needed for such computations. Provisions for addition of neurons at learning-rate-threshold levels could be made easily in hardware.

This work was done by Tuan A. Duong of Caltech for NASA's Jet Propulsion Laboratory. Further information is contained in a TSP (see page 1).

This invention is owned by NASA, and a patent application has been filed. Inquiries concerning nonexclusive or exclusive license for its commercial development should be addressed to the Patent Counsel, NASA Management Office-JPL; (818) 354-7770. Refer to NPO-19289.



Perovskite Superlattices as Tunable Microwave Devices

Interfacial interactions between paraelectric materials induce quasi-ferroelectric behavior.

John H. Glenn Research Center, Cleveland, Ohio

Experiments have shown that superlattices that comprise alternating epitaxial layers of dissimilar paraelectric perovskites can exhibit large changes in permittivity with the application of electric fields. The superlattices are potentially useful as electrically tunable dielectric components of such microwave devices as filters and phase shifters.

The electrically tunable materials heretofore used in some microwave devices exhibit strong temperature dependences of dielectric properties and high microwave losses. Previous efforts to overcome these undesired effects have involved the addition of various dopants to SrTiO_3 , BaTiO_3 , and $\text{Sr}_x\text{Ba}_{1-x}\text{TiO}_3$. Despite the amount of research in this area, results have been disappointing.

The present superlattice approach differs fundamentally from the prior use of homogeneous, isotropic mixtures of

base materials and dopants. A superlattice can comprise layers of two or more perovskites in any suitable sequence (e.g., ABAB..., ABCDABCD..., ABCABACA...). Even though a single layer of one of the perovskites by itself is not tunable, the compositions and sequence of the layers can be chosen so that (1) the superlattice exhibits low microwave loss and (2) the interfacial interaction between at least two of the perovskites in the superlattice renders either the entire superlattice or else at least one of the perovskites tunable.

The perovskites investigated experimentally for use in superlattices include SrTiO_3 , SrCeO_3 , SrZrO_3 , BaTiO_3 , BaZrO_3 , CaZrO_3 , and LaAlO_3 . Superlattices for the experiments were fabricated by pulsed laser deposition onto mostly LaAlO_3 substrates; a few specimens were prepared on SrTiO_3 substrates. Microwave filters containing superlattices were also fabricated. The

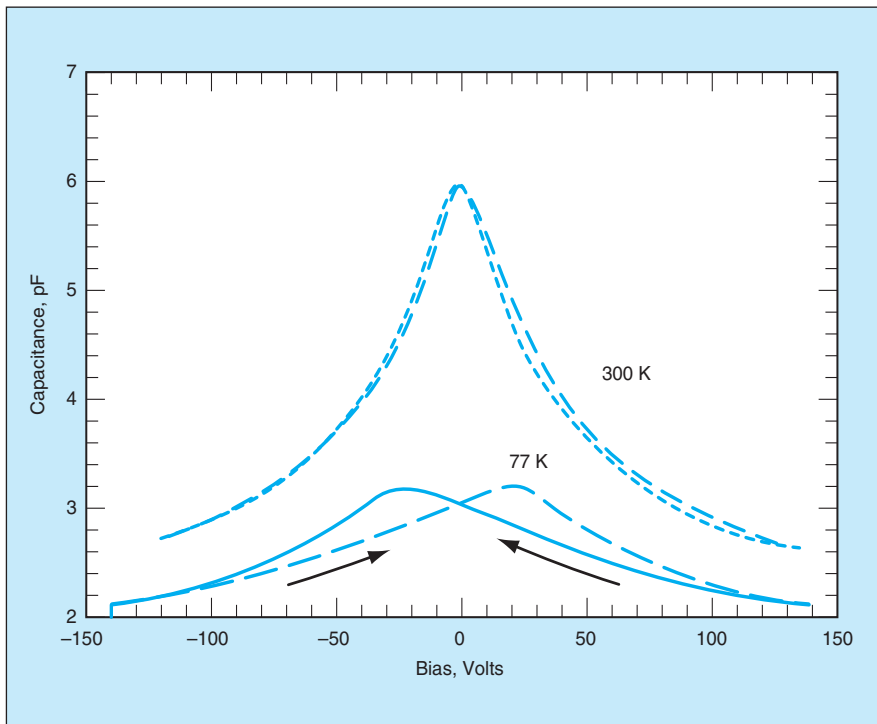
superlattices were evaluated with respect to structure, composition, and dielectric properties.

Analysis of the observations made in the experiments led to the following conclusions:

- Large tuning was observed in capacitors made from some superlattices (see figure). Ferroelectricity induced by lattice-mismatch strain in superlattices has been tentatively identified as the cause of tunability in the otherwise nontunable paraelectric perovskite constituents.
- Some of the superlattices exhibited positive $d\epsilon/dE$, where ϵ is permittivity and E is the magnitude of an applied electric field. This stands in contrast to the negative values of $d\epsilon/dE$ typically observed in perovskites.
- Superlattices can be made to exhibit weak temperature dependences of tunability. For example, one $\text{SrTiO}_3/\text{BaZrO}_3$ superlattice was found to exhibit a tunability of 33 percent at both room temperature and at 77 K. In contrast, a typical ferroelectric material is tunable in only a narrow temperature range near a phase transition. Superlattices with weak temperature dependence of tunability could be attractive materials for situations in which precise control of temperature would be either impossible or too expensive.
- In tests on coplanar-waveguide microwave filters containing perovskite superlattices of a given total thickness, dielectric losses were found to be smaller than those in filters containing single SrTiO_3 films of the same total thickness.

This work was done by H. M. Christen and K. S. Harshavardhan of Neocera, Inc., for Glenn Research Center. Further information is contained in a TSP (see page 1).

Inquiries concerning rights for the commercial use of this invention should be addressed to NASA Glenn Research Center, Commercial Technology Office, Attn: Steve Fedor, Mail Stop 4-8, 21000 Brookpark Road, Cleveland, Ohio 44135. Refer to LEW-16938.



Tunability in Excess of 50 Percent was observed in a capacitor in which the dielectric was a superlattice of $\text{SrTiO}_3/\text{CaZrO}_3$ with layer thicknesses chosen for large tunability at room temperature.

Rollable Thin-Shell Nanolaminate Mirrors

Advanced concepts of actuation, control, and materials are combined.

NASA's Jet Propulsion Laboratory, Pasadena, California

A class of lightweight, deployable, thin-shell, curved mirrors with built-in precise-shape-control actuators is being developed for high-resolution scientific imaging. This technology incorporates a combination of advanced design concepts in actuation and membrane optics that, heretofore, have been considered as separate innovations. These mirrors are conceived to be stowed compactly in a launch shroud and transported aboard spacecraft, then deployed in outer space to required precise shapes at much larger dimensions (diameters of the order of meters or tens of meters).

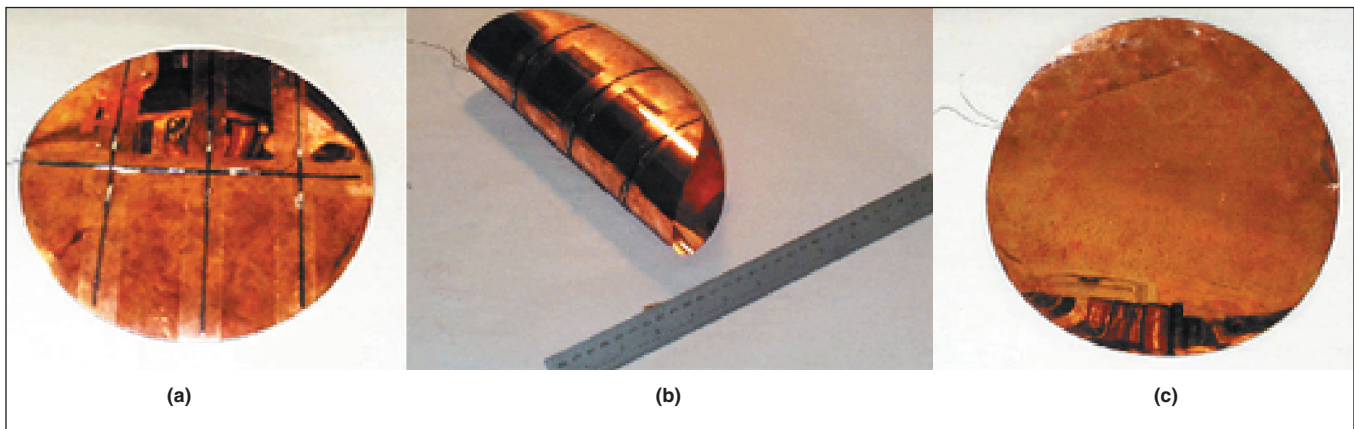
A typical shell rollable mirror structure would include (1) a flexible single- or multiple-layer face sheet that would include an integrated reflective surface layer that would constitute the mirror; (2) structural supports in the form of stiffeners made of a shape-memory alloy (SMA); and (3) piezoelectric actuators. The actuators, together with an electronic control subsystem, would imple-

ment a concept of hierarchical distributed control, in which (1) the SMA actuators would be used for global shape control and would generate the large deformations needed for the deployment process and (2) the piezoelectric actuators would generate smaller deformations and would be used primarily to effect fine local control of the shape of the mirror.

Another advanced design concept is that of nanolaminate mirror shells. This design concept builds upon technology reported previously in "Nanolaminate Mirrors With Integral Figure-Control Actuators" (NPO-30221), *NASA Tech Briefs*, Vol. 26, No. 5 (May 2002), page 80. Nanolaminates constitute a relatively new class of materials that can approach theoretical limits of stiffness and strength. For making the proposed mirrors, nanolaminates are synthesized by magnetron sputter deposition of metallic alloys and/or compounds on optically precise master surfaces to obtain an optical-quality reflector. Ideally, the

crystallographic textures of the deposited layers would be controlled to optimize mechanical performance. The present development efforts are directed toward incorporating the nanolaminate concept into the first-mentioned concept of the deployable shell structure with built-in SMA and piezoelectric shape-control actuators. In a typical intended application, a thin-shell paraboloidal mirror would be stowed by rolling it into a taco or cigar shape. Subsequently, it would be deployed by use of its SMA, which would "remember" the unrolled shape. As shown in the figure, the feasibility of this stowage/deployment concept was verified in an experiment.

This work was done by Gregory Hickey and Shyh-Shiuh Lih of Caltech and Troy Barbee, Jr., of Lawrence Livermore National Laboratory for NASA's Jet Propulsion Laboratory. Further information is contained in a TSP (see page 1). NPO-30214



SMA Ribbons (a) were trained to 2-m radius of curvature and then bonded to the rear surface of a nanolaminate substrate 25 cm in diameter and 100 μm thick. The nanolaminate (b) was then rolled as though for stowage. Next, when an electric current was applied to heat the SMA ribbons, the substrate returned from the rolled-up configuration to its original 2-m radius of curvature (c).



✈ Flight Tests of a Ministick Controller in an F/A-18 Airplane

Pilots' opinions were generally favorable.

Dryden Flight Research Center, Edwards, California

In March of 1999, five pilots performed flight tests to evaluate the handling qualities of an F/A-18 research airplane equipped with a small-displacement center stick (ministick) controller that had been developed for the JAS 39 Gripen airplane (a fighter/attack/reconnaissance airplane used by the Swedish air force). For these tests, the ministick was installed in the aft cockpit (see figure) and production support flight control computers (PSFCCs) were used as interfaces between the controller hardware and the standard F/A-18 flight-control laws.

The primary objective of the flight tests was to assess any changes in handling qualities of the F/A-18 airplane attributable to the mechanical characteristics of the ministick. The secondary objective was to demonstrate the capability of the PSFCCs to support flight-test experiments.

The ministick, together with an associated demodulator box, generated single-channel pitch and roll stick commands in the form of DC signals, which were fed to analog input terminals of the PSFCCs. Software was developed to effect cross-channel data links, error detection of signals, and scaling of commands. The signals were scaled to be similar to the maximum inputs generated by the standard F/A-18 control stick. Because the experiment was to assess the effects of the mechanical characteristics of a small-displacement, center-mounted control stick, the original deadbands and stick shaping were used.

The five pilots performed five test flights. General comments and ratings of handling quali-



The **Ministick** is shown here installed in the aft cockpit of the F/A-18 airplane.

ties were collected. The tests included the following maneuvers: doublets, frequency sweeps, bank attitude captures, pitch attitude captures, echelon formation flight, column formation flight, gross acquisition, and fine tracking. The echelon formation flight comprised three phases: gentle maneuvering, vertical captures, and more aggressive ma-

neuvvers. The column formation flight also comprised three phases: gentle maneuvers, more aggressive maneuvers, and lateral captures.

Cooper-Harper ratings are summarized in the table. The pilots consistently noted that the stick was very sensitive in roll, with some tendency to ratcheting. This tendency could be mitigated by modifying the stick shaping and deadband. The general pilots' comments on the ministick were favorable. The pilots noted that it was extremely easy to generate full-amplitude inputs. At the time of reporting the information for this article, analysis of data was nearing completion and technical reports to document the flight test, compare results with handling-qualities criteria, and describe the process of testing and operating the PSFCCs were in preparation.

This work was done by Patrick C. Stoliker and John Carter of Dryden Flight Research Center. For more information, contact the Dryden Commercial Technology Office at 661-276-3689. DRC-01-33

Pilot	A	B	C	D	E
Echelon Formation Phase 1	4	3	2	3	3
Echelon Formation Phase 2	4	5	3	2	4
Echelon Formation Phase 3	4 to 7	5	4	4	5
Column Formation Phase 1	4	3	2	4	4
Column Formation Phase 2	3	3	2	4	5
Column Formation Phase 3	3 to 4	5	5	4	4
Gross Acquisition	n/a	6 to 7	2	2	4
Longitudinal Fine Tracking	n/a	3	2	2	3
Lateral Fine Tracking	n/a	4	2	3	6

Handling Qualities are summarized here on the Cooper-Harper scale (named after the authors of a 1986 paper on ratings of handling qualities by pilots).

Piezoelectrically Actuated Shutter for High Vacuum

This vacuum-compatible shutter generates an acceptably small magnetic field.

NASA's Jet Propulsion Laboratory, Pasadena, California

A piezoelectrically actuated shutter is undergoing development for use in experiments on laser cooling of atoms. The shutter is required to be compatible with ultrahigh vacuum [pressure of 10^{-9} torr

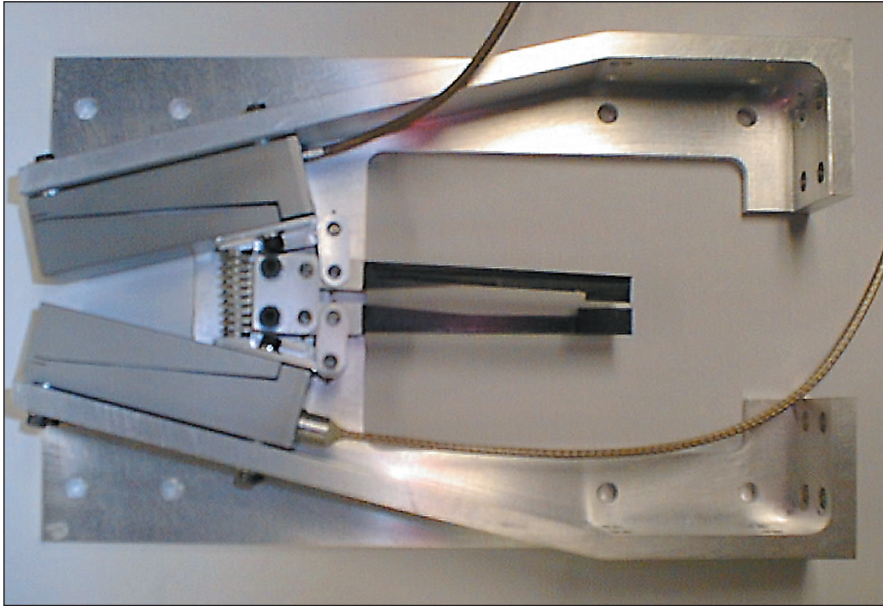
($\approx 1.3 \times 10^{-7}$ Pa) or less] and to be capable of performing reliably in the vacuum for at least one year. In operation, the shutter would enable the collection and launch of successive samples of cold atoms and

would enable the interrogation of the immediately preceding sample while preventing disturbance of the atoms of that sample by light from the collection region.

A major constraint is imposed on the design and operation of the shutter by a requirement that it not generate a magnetic field large enough to perturb an atomic clock. An electromagnetically actuated shutter could satisfy all requirements except this one. Hence, it was decided to use piezoelectric instead of electromagnetic actuation.

The shutter (see figure) includes two commercial piezoelectrically driven flexure stages that produce a travel of 0.5 mm. Levers mechanically amplify the travel to the required level of 1 cm. Problems that remained to be addressed at the time of reporting the information for this article included lifetime testing and correction of a tendency for shutter blades to bounce open.

This work was done by Robert Thompson and Gerhard Klose of Caltech for NASA's Jet Propulsion Laboratory. Further information is contained in a TSP (see page 1). NPO-30397



This is a **Prototype of the Shutter** under development for use in experiments on laser cooling of atoms.

Bio-Inspired Engineering of Exploration Systems

Exploration systems with capabilities imbibed from nature enable new operations that were otherwise very difficult or impossible to accomplish.

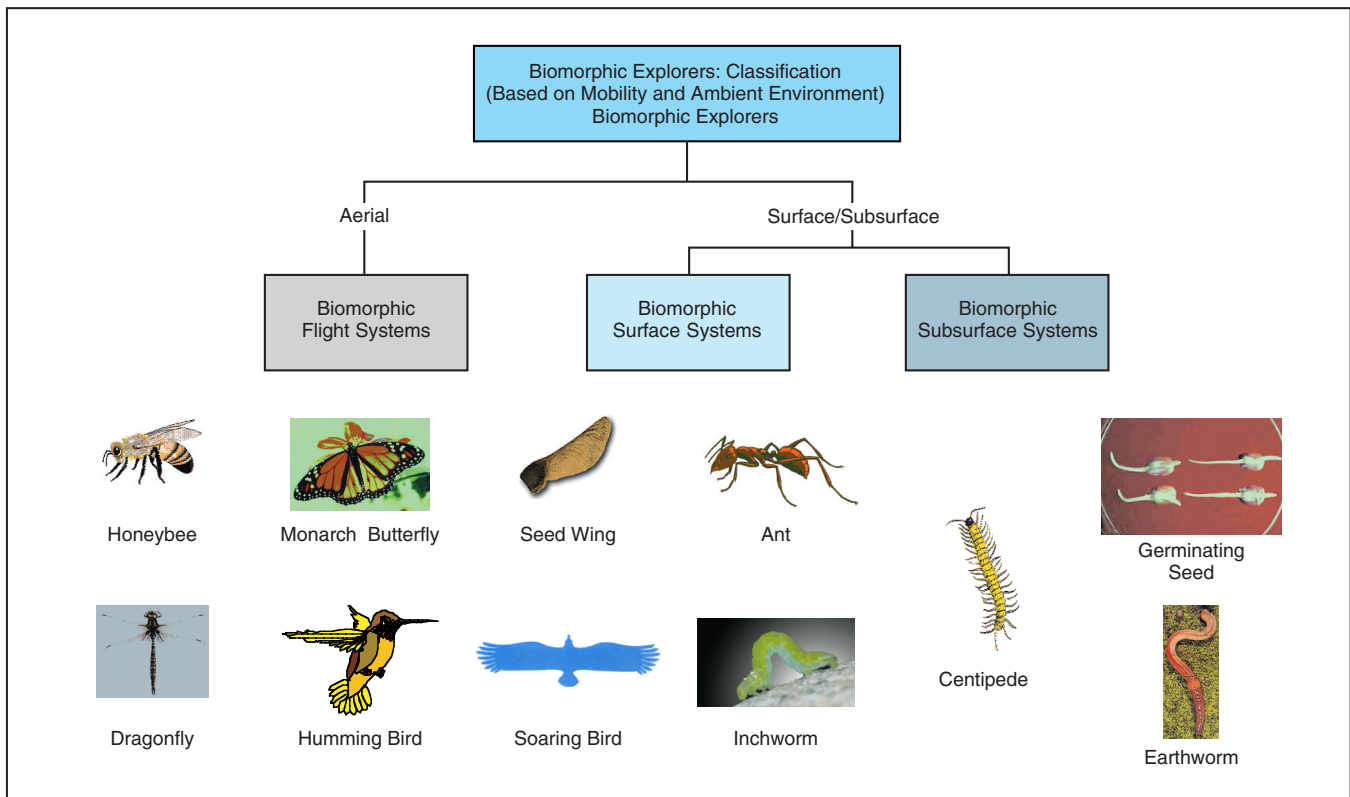
NASA's Jet Propulsion Laboratory, Pasadena, California

The multidisciplinary concept of “bioinspired engineering of exploration systems” (BEES) is described, which is a guiding principle of the continuing effort to develop biomorphic explorers as reported in a number of articles in the past issues of *NASA Tech Briefs*. The intent of BEES is to distill from the principles found in successful nature-tested mechanisms of specific “crucial functions” that are hard to accomplish by conventional methods but that are accomplished rather deftly in nature by biological organisms. The intent is not just to mimic operational mechanisms found in a specific biological organism but to imbibe the salient principles from a variety of diverse bio-organisms for the desired “crucial function.” Thereby, we can build explorer systems that have specific capabilities endowed beyond nature, as

they will possess a combination of the best nature-tested mechanisms for that particular function. The approach consists of selecting a crucial function, for example, flight or some selected aspects of flight, and develop an explorer that combines the principles of those specific attributes as seen in diverse flying species into one artificial entity. This will allow going beyond biology and achieving unprecedented capability and adaptability needed in encountering and exploring what is as yet unknown. A classification of biomorphic flyers into two main classes of surface and aerial explorers is illustrated in the figure, with examples of a variety of biological organisms that provide the inspiration in each respective subclass.

Such biomorphic explorers may possess varied mobility modes: surface-rov-

ing, burrowing, hopping, hovering, or flying, to accomplish surface, subsurface, and aerial exploration. Preprogrammed for a specific function, they could serve as one-way communicating beacons, spread over the exploration site, autonomously looking for/at the targets of interest. In a hierarchical organization, these biomorphic explorers would report to the next level of exploration mode (say, a large conventional lander/rover) in the vicinity. A widespread and affordable exploration of new/hazardous sites at lower cost and risk would thus become possible by utilizing a faster aerial flyer to cover long ranges and deploying a variety of function-specific, smaller biomorphic explorers for distributed sensing and local sample acquisition. Several conceptual biomorphic missions for plane-



These Examples of Biological Inspirations show different mobility categories.

tary and terrestrial exploration applications have been illustrated in "Surface-Launched Explorers for Reconnaissance/Scouting" (NPO-20871), *NASA Tech Briefs*, Vol. 26, No. 4 (April, 2002), page 69 and "Bio-Inspired Engineering of Exploration Systems," *Journal of Space Mission Architecture*, Issue 2, Fall 2000, pages 49-79.

Insects (for example, honey bees and dragonflies) cope remarkably well with their world, despite possessing a brain that carries less than 0.01 percent as many neurons as that of the human. Although most insects have immobile eyes, fixed-focus optics, and lack stereo vision, they use a number of ingenious strategies for perceiving their world in three dimensions and navigating successfully in it. We are distilling some of these insect-inspired strategies to obtain unique solutions to navigation, hazard avoidance, terrain following, and smooth deployment of payload. Such functionality

can enable one to reach previously unreachable exploration sites.

In-situ, autonomous exploration and science return from planetary surfaces and subsurfaces would be substantially enhanced if a large number of small, inexpensive, and therefore dispensable, biomorphic explorers equipped with dedicated microsensors could be spread over the surface. Their low-cost and small size would make them ideal for hazardous or difficult site exploration, inspection, and testing. Their dedicated sensing functions and autonomous maneuverability would be valuable in scouting missions and sample acquisition from hard-to-reach places. As was mentioned earlier, when preprogrammed for a specific function and spread over the exploration site, these explorers could serve as intelligent, downlink-only beacons that autonomously look for objects of interest. Alternatively, these biomorphic explorers can operate in a hierar-

chical organization and report their findings to the next higher level of exploration (say, a large conventional lander/rover) in the vicinity. Specifically, our recent results demonstrate the novelty of our approach in adapting principles proven successful in nature to achieve stable flight control, navigation, and visual search/recognition. This approach has enabled overall a robust architecture for reliable image data return in application scenarios both for terrestrial and planetary needs where only a limited telecommunications or navigational infrastructure is available and is therefore otherwise by traditional methods hard or impossible to explore.

*This work was done by Sarita Thakoor of Caltech for NASA's Jet Propulsion Laboratory. Further information is contained in a TSP (see page 1).
NPO-21142*

Microscope Cells Containing Multiple Micromachined Wells

The cost per cell has been reduced substantially.

John H. Glenn Research Center, Cleveland, Ohio

An improved design for multiple-well microscope cells and an associated improved method of fabricating them have been devised. [As used here, “well” denotes a cavity that has a volume of about 1 or 2 μL and that is used to hold a sample for examination under a microscope. As used here, “cell” denotes a laminate, based on a standard 1- by 3-in. (2.54- by 7.62-cm) microscope slide, that comprises (1) the slide as the lower layer, (2) an intermediate layer that contains holes that serve as the wells, and (3) a top layer that either consists of, or is similar to, a standard microscope-slide cover slip.] The improved design and method of fabrication make it possible to increase (relative to a prior design and method of fabrication) the number of wells per cell while reducing the fabrica-

tion loss and reducing the cost per cell to about one-tenth of the prior value.

In the prior design and method, the slide, well, and cover-slip layers were made from silicate glass. The fabrication of each cell was a labor-intensive process that included precise cutting and grinding of the glass components, fusing of the glass components, and then more grinding and polishing to obtain desired dimensions. Cells of the prior design were expensive and fragile, the rate of loss in fabrication was high, and the nature of the glass made it difficult to increase the number of cells per well. Efforts to execute alternative prior designs in plastic have not yielded satisfactory results because, for typical applications, plastics are not sufficiently thermally or chemically stable, not sufficiently opti-

cally clear, and/or not hard enough to resist scratching.

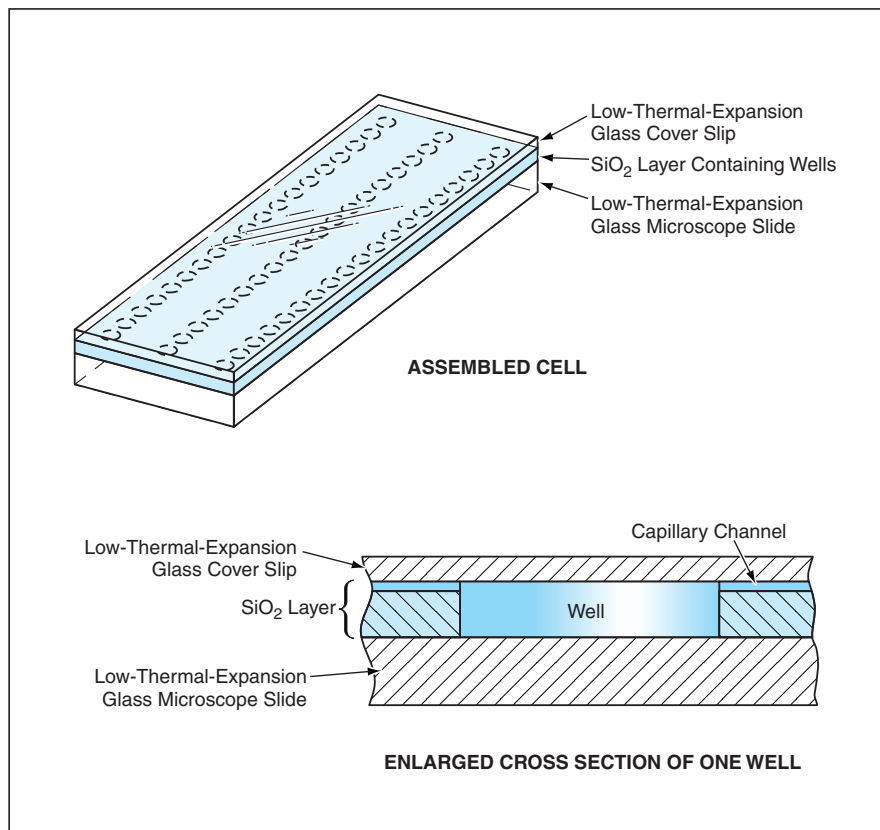
The figure depicts a cell of the present improved type. The slide and cover-slip layers are made of a low-thermal-expansion glass (Pyrex™ or equivalent) and the intermediate (well layer) is made of SiO_2 — a combination of materials that results in a laminate stronger than one made from layers of silicate glass. Before the layers are assembled into the laminate, the SiO_2 layer is micromachined to form the wells plus shallow grooves that, when subsequently covered with the cover slip, become capillary channels that are used to fill the wells with samples. The micromachining is accomplished by use of the same patterning and etching techniques used to fabricate microelectromechanical systems (MEMS).

Typically the thickness of the SiO_2 layer must be made $\leq 200 \mu\text{m}$ — a requirement dictated by the viewing characteristics of the microscope and the nature of the microscopic examination to be performed. Prior to assembly into the laminate, the slide and cover-slip layers should be optically clear and should be polished to a tolerance tight enough to enable electrostatic bonding to the well layer.

Once the cell has been assembled, each well is filled with a sample through one of its capillary channels. Then an ultraviolet-curing epoxy is wicked into all the capillary channels, and the cell is exposed to ultraviolet light to cure the epoxy and thereby seal the samples into the wells. The cell is then ready for examination under a microscope.

This work was done by Walter Turner and Robert Skupinski of Dynacs Engineering Co., Inc., for Glenn Research Center. Further information is contained in a TSP (see page 1).

Inquiries concerning rights for the commercial use of this invention should be addressed to NASA Glenn Research Center, Commercial Technology Office, Attn: Steve Fedor, Mail Stop 4-8, 21000 Brookpark Road, Cleveland, Ohio 44135. Refer to LEW-17016.



Three Layers Are Electrostatically Bonded to produce a laminated multiple-well sample cell with capillary channels for filling the wells.

Electrophoretic Deposition for Fabricating Microbatteries

Discharge capacities can be much greater than those achieved previously.

NASA's Jet Propulsion Laboratory, Pasadena, California

An improved method of fabrication of cathodes of microbatteries is based on electrophoretic deposition. Heretofore, sputtering (for deposition) and the use of photoresist and liftoff (for patterning) have been the primary methods of fabricating components of microbatteries. The volume of active electrode material that can be deposited by sputtering is limited, and the discharge capacities of prior microbatteries have been limited accordingly. In addition, sputter deposition is slow. In contrast, electrophoretic deposition is much faster and has shown promise for increasing discharge capacities by a factor of 10, relative to those of microbatteries fabricated by prior methods.

Microbatteries of the type to which the improved method applies are fabricated on silicon wafers, with cell footprints of the order of $(50 \text{ to } 100 \mu\text{m})^2$. In the improved method, cathodes are formed directly on cathode current-collector pads; there is no need for additional lithogra-

phy or etching to define the cathodes. In order to make it possible for cathode material to be deposited onto current-collector pads, it is necessary to ensure that the pads are electrically connected to ground during the electrophoretic deposition process. This can be done in any of several different ways. For example, current collectors can be deposited by sputtering and patterned such that a metal line connects all current collectors. After electrophoretic deposition of cathode material, the connecting lines can be removed by simple patterning and etching to yield unconnected microbattery cells.

Alternatively, in a simpler approach that has been followed in practical development thus far, an electrically conductive silicon substrate can be used as a ground plane. First, a silicon wafer is coated with an insulating layer of silicon dioxide or silicon nitride to a thickness of about 3 to 5 μm . The substrate is patterned with photoresist and subjected

to reactive-ion etching to open vias to the silicon substrate. These vias serve the cathode current collectors for the microbattery. The exposed silicon can then be further etched to produce deep pockets into which cathode material can be deposited to increase the effective volume of cathode material (see figure).

A suspension of powdered cathode material (e.g., LiCoO_2), acetone, iodine, and an electrically conductive additive is prepared. The iodine serves to facilitate the formation of positively charged complexes of the particles to be deposited so that they can be moved through the applied electric field during deposition. The conductive additive could be, for example, tin powder or carbon black.

The substrate is positioned about 1 cm from a counter electrode. The substrate/counter-electrode assembly is immersed in the suspension, and then a potential of about 70 V is applied between the substrate and the counter electrode (the counter electrode being positive with respect to the substrate) for a time of about 90 seconds. The particles of cathode material, being positively charged, are transported through the suspension to the silicon substrate, where they become deposited only on electrically conductive surfaces. The substrates are then coated with a solid-electrolyte film and patterned with anode current collectors by use of previously published techniques.

This work was done by William West, Jay Whitacre, and Ratnakumar Bugga of Caltech for NASA's Jet Propulsion Laboratory. Further information is contained in a TSP (see page 1).

In accordance with Public Law 96-517, the contractor has elected to retain title to this invention. Inquiries concerning rights for its commercial use should be addressed to

Intellectual Assets Office

JPL

Mail Stop 202-233

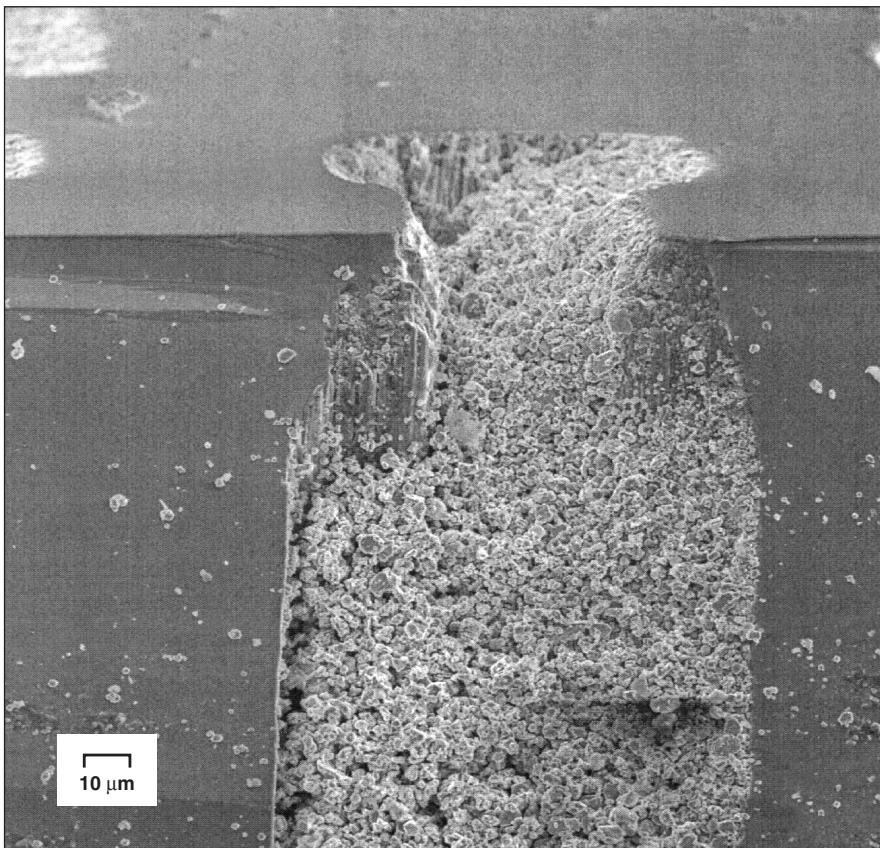
4800 Oak Grove Drive

Pasadena, CA 91109

(818) 354-2240

E-mail: ipgroup@jpl.nasa.gov

Refer to NPO-30394, volume and number of this NASA Tech Briefs issue, and the page number.



Particles of LiCoO_2 and ancillary cathode constituents were deposited into microscopic holes etched into a silicon substrate. This is a cross-sectional view of one of the holes.

Integrated Arrays of Ion-Sensitive Electrodes

Electronic “tongues” would “taste” selected ions in water.

NASA’s Jet Propulsion Laboratory, Pasadena, California

The figure depicts an example of proposed compact water-quality sensors that would contain integrated arrays of ion-sensitive electrodes (ISEs). These sensors would serve as electronic “tongues”: they would be placed in contact with water and used to “taste” selected dissolved ions (that is, they would be used to mea-

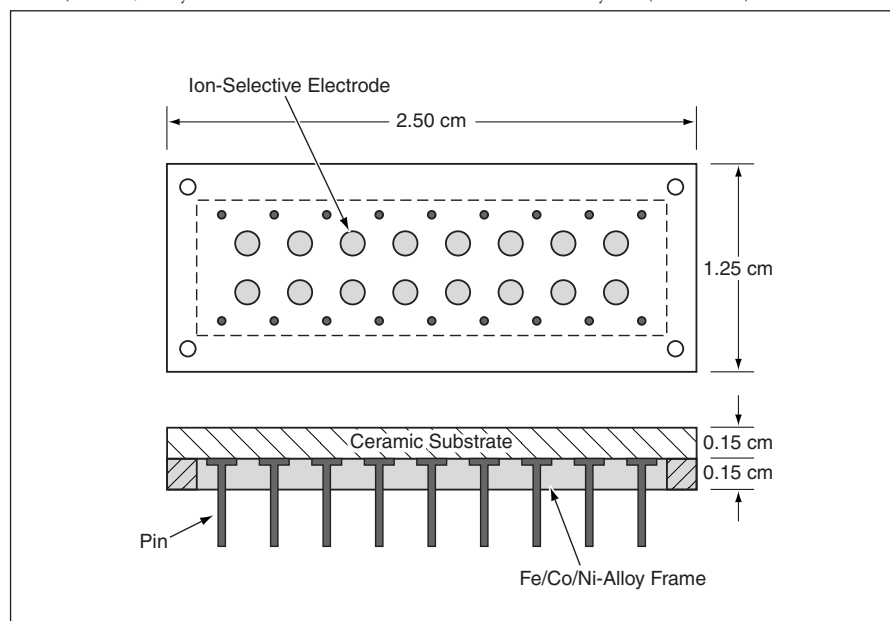
sure the concentrations of the ions). The selected ions could be any or all of a variety of organic and inorganic cations and anions that could be regarded as contaminants or analytes, depending on the specific application. In addition, some of the ISEs could be made sensitive to some neutral analytes (see table).

Discrete ISEs are commercially available, but are large, relative to the ISEs in the proposed sensors. In comparison with an array of commercial ISEs, an array of the proposed type would be about ten times as dense; in other words, one could detect a greater variety of ions by use of a sensor of a given size, or, alternatively, the sensor needed to detect a given set of ionic species could be made smaller. In addition, the proposed sensors have been conceptually designed to be amenable to mass production at relatively low cost.

In the example of the figure, the array of ISEs would be formed on a co-fired ceramic substrate strengthened by a Kovar (or equivalent) iron/nickel/cobalt-alloy frame. Each electrode would comprise a gel layer covered by a polymer layer and further covered by a protective layer. Fabrication of the array would include the following sequence of operations:

1. The gel layers of the electrodes would be deposited on the substrate by screen printing.
2. By use of an electrolytic doping apparatus, each electrode would be doped electrostatically with a selected ionophore. The basic principle of the doping process would be similar to that of electrophoresis, wherein molecular fragments migrate along a conductive gel channel under the influence of an electric field. The design and mode of operation of the apparatus would be such that the process of doping each electrode would not deplete previously doped electrodes.
3. The polymer layers of the electrodes would be deposited by screen printing in the same manner as that of the gel layers.
4. The polymer layers would be doped in the same manner as that of the gel layers.
5. The protective layers would be screen-printed over the electrodes.

The sensor would be inserted in a socket on a printed-circuit board that would contain electronic circuitry for



A Unitary Array of 16 ISEs would occupy an area of only about 3.1 cm². An array of 16 discrete ISEs would be much larger.

Inorganic Cations	H ⁺ , Li ⁺ , Na ⁺ , K ⁺ , Rb ⁺ , Cs ⁺ , Be ²⁺ , Mg ²⁺ , Ca ²⁺ , Sr ²⁺ , Ba ²⁺ , Mo ⁴⁺ , Fe ³⁺ , Cu ²⁺ , Ag ⁺ , Zn ²⁺ , Cd ²⁺ , Hg ²⁺ , Tl ⁺ , Bi ³⁺ , Pb ²⁺ , U ⁴⁺ , Sm ³⁺ , NH ⁴⁺
Inorganic Anions	CO ₃ ²⁻ , HCO ₃ ⁻ , SCN ⁻ , NO ₂ ⁻ , OH ⁻ , phosphate, sulfite, SO ₄ ²⁻ , Cl ⁻ , SeO ₃ ²⁻ , I ⁻
Organic Cations	1-phenylethylamine, 1-(1-naphthyl)-ethylamine, ephedrine, norephedrine, pseudoephedrine, amphetamine, propanolol, amino acid methyl esters, α-amino-ε-caprolactam, amino acid amides, benzyl amine, alkyl amines, dopamine, mexiletine, local anesthetics (procaine, prilocaine, lidocaine, bupivacaine, lignocaine), diquat and paraquat (herbicides), tetramethyl- and tetraethylammonium, guanidine, metformin, phenformin, creatinine, protamine
Organic Anions	salicylate, phthalate, maleate, 2-hydroxybenzhydroxamate, nucleotides, heparin
Neutral Analytes	CO ₂ , O ₂ , NH ₃

These **Ions and Neutral Analytes** are ones for which ionophores have been reported and for which ISEs are expected to exhibit (1) linear responses at concentrations up to 1 M and (2) sensitivity to concentrations as low as 10⁻⁶ M.

processing the ISE outputs. The circuitry would include analog-to-digital converters measuring the ISE potentials. The circuitry would also include digital multiplexers for transmitting the potentials to a computer, which would analyze the potentials to determine the concentrations of ions of the selected species.

This work was done by Martin Buehler and Kimberly Kuhlman of Caltech for NASA's Jet Propulsion Laboratory. Further information is contained in a TSP (see page 1).

In accordance with Public Law 96-517, the contractor has elected to retain title to this invention. Inquiries concerning rights for its commercial use should be addressed to

*Intellectual Property group
JPL
Mail Stop 202-233
4800 Oak Grove Drive
Pasadena, CA 91109
(818) 354-2240*

Refer to NPO-20700, volume and number of this NASA Tech Briefs issue, and the page number.

Model of Fluidized Bed Containing Reacting Solids and Gases

This model can be used to optimize designs and operating conditions.

NASA's Jet Propulsion Laboratory, Pasadena, California

A mathematical model has been developed for describing the thermofluid dynamics of a dense, chemically reacting mixture of solid particles and gases. As used here, "dense" signifies having a large volume fraction of particles, as for example in a bubbling fluidized bed. The model is intended especially for application to fluidized beds that contain mixtures of carrier gases, biomass undergoing pyrolysis, and sand. So far, the design of fluidized beds and other gas/solid industrial processing equipment has been based on empirical correlations derived from laboratory- and pilot-scale units. The present mathematical model is a product of continuing efforts to develop

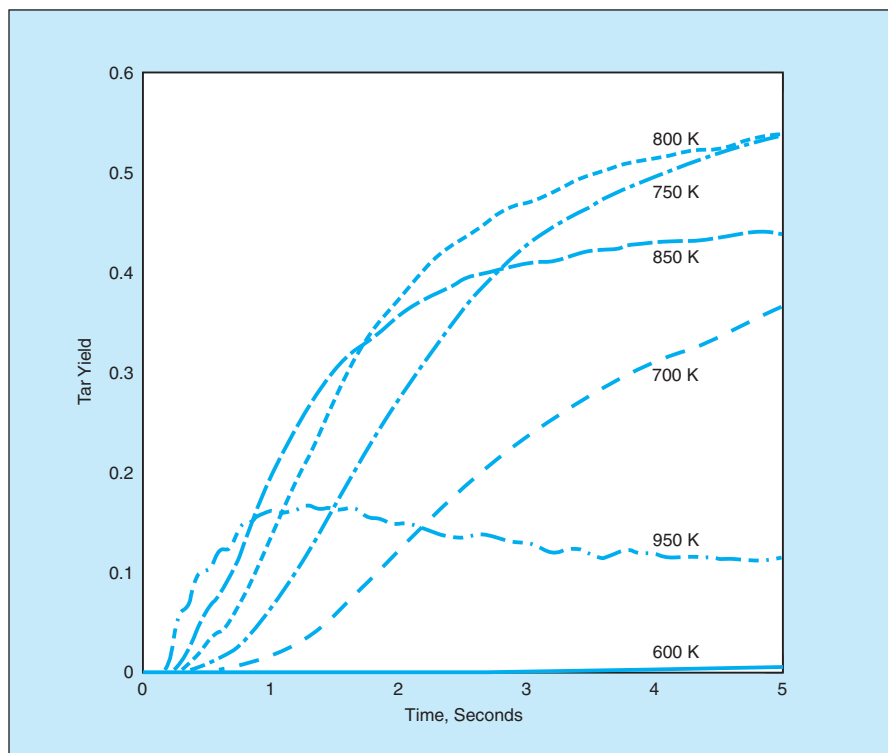
a computational capability for optimizing the designs of fluidized beds and related equipment on the basis of first principles. Such a capability could eliminate the need for expensive, time-consuming predesign testing.

The present model includes components in common with models described in several previous *NASA Tech Briefs* articles, including, most notably, "Model of Pyrolysis of Biomass in a Fluidized-Bed Reactor" (NPO-20708), *NASA Tech Briefs*, Vol. 25, No. 6 (June 2001), page 59; "Multiphase-Flow Model of Fluidized-Bed Pyrolysis of Biomass" (NPO-20789), *NASA Tech Briefs*, Vol. 26, No. 2 (February 2002), page 56; and "Model of a Flu-

idized Bed Containing a Mixture of Particles" (NPO-20937), *NASA Tech Briefs*, Vol. 26, No. 4 (April 2002), page 56. The model distinguishes among multiple particle classes on the basis of physical properties (e.g., diameter or density) and/or through thermochemical properties (e.g., chemical reactivity or nonreactivity). The formulation of the model follows a multifluid approach in which macroscopic equations for the solid phase are derived from a kinetic-like theory considering inelastic-rigid-sphere submodels in accounting for collisional transfer in high-density regions. The gas phase equations are derived using ensemble averaging.

Separate transport equations are constructed for each of the particle classes, providing for the separate description of the acceleration of the particles in each class, of interactions between particles in different size classes, and of the equilibration processes in which momentum and energy are exchanged among the particle classes and the carrier gas. The kinetic-like theory is based on a Gaussian approximation of the velocity distribution, assuming that spatial gradients of mean variables are small and particles are nearly elastic. Each class of particles is characterized by its own granular temperature, which represents the mean kinetic energy associated with fluctuations in the velocities of the particles. The stress tensor is augmented by a frictional-transfer submodel of stress versus strain: The separate equations of the dynamics of the various particle classes are coupled through source terms that describe such nonequilibrium processes as transfer of mass, momentum, and energy, both between particles and between gas and particles.

In one of several test cases, the model was applied to the pyrolysis of biomass



The Tar Yield of a Fluidized Bed as a function of time was computed, for various temperatures of fluidizing gas, by use of the model described in the text.

particles in a laboratory fluidized bed reactor and used to compute yields of reaction products (especially tar). The results indicate that at fixed initial particle size, the temperature of the fluidizing gas is the foremost parameter that influ-

ences the tar yield and can be chosen to maximize the tar yield (see figure). The temperature of the biomass feed, the nature of the feedstock, and the fluidization velocity were all found to exert only minor effects on the tar yield.

*This work was done by Josette Bellan and Danny Lathouwers of Caltech for NASA's Jet Propulsion Laboratory. Further information is contained in a TSP (see page 1).
NPO-30163*

Membrane Mirrors With Bimorph Shape Actuators

Only modest control voltages would be needed.

NASA's Jet Propulsion Laboratory, Pasadena, California

Deformable mirrors of a proposed type would be equipped with relatively large-stroke microscopic piezoelectric actuators that would be used to maintain their reflective surfaces in precise shapes. These mirrors would be members of the class of MEMS-DM (for microelectromechanical system deformable mirror) devices, which offer potential for a precise optical control in adaptive-optics applications in such diverse fields as astronomy and vision science.

In some respects, the proposed mirrors would be similar to the ones described in "Silicon Membrane Mirrors With Electrostatic Shape Actuators" (NPO-21120) *NASA Tech Briefs*, Vol. 27, No. 1 (January 2003), page 62. Like a mirror of the type reported previously,

a mirror as proposed here would include a continuous-membrane reflector attached by posts to actuators that, in turn, would be attached by posts to a rigid base (see figure). Also as before, the proposed mirror would be fabricated, in part, by use of a membrane-transfer technique. However, the actuator design would be different. Instead of the electrostatic actuators reported previously, the proposed mirror would contain bimorph-type piezoelectric actuators.

The reasons for the proposed choice of actuators are simple: In the mirror described in the cited prior article as well as in other previously reported membrane mirrors that feature piezoelectric and electrostrictive actuators, it is not possible, by use of mod-

est actuation voltages, to obtain actuator strokes of the order of $\pm 6 \mu\text{m}$ as needed in the intended adaptive-optics applications. The mechanical amplification inherent in the bimorph configuration would multiply the small displacements typically generated by piezoelectric devices, thereby making it possible to obtain the desired stroke magnitudes at voltages lower than would be needed to obtain the same stroke magnitudes from non-bimorph piezoelectric and electrostatic actuators.

A voltage applied to the piezoelectric layer in a given actuator would induce a stress that would cause the actuator layer to bend and thus to pull or push on the mirror membrane. It has been estimated that an applied potential of $\pm 9 \text{ V}$ should be sufficient to produce an actuator stroke, and thus a local reflector displacement, of $\pm 6 \mu\text{m}$. Inasmuch as the actuators would be essentially capacitors from an electrical perspective, the actuators would consume power only during changes in their position settings. During maintenance of a position setting, only the supporting electronic circuitry would consume power.

This work was done by Eui-Hyeok Yang of Caltech for NASA's Jet Propulsion Laboratory. Further information is contained in a TSP (see page 1).

In accordance with Public Law 96-517, the contractor has elected to retain title to this invention. Inquiries concerning rights for its commercial use should be addressed to

Intellectual Property group

JPL

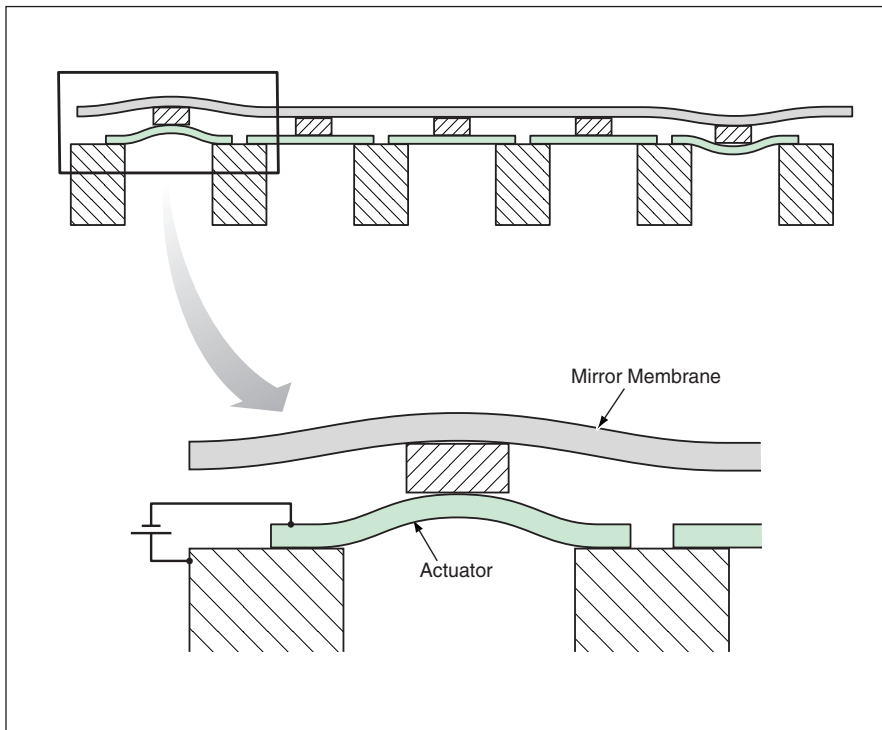
Mail Stop 202-233

4800 Oak Grove Drive

Pasadena, CA 91109

(818) 354-2240

Refer to NPO-30230, volume and number of this NASA Tech Briefs issue, and the page number.



This **Deformable Mirror** would contain bimorph actuators, which would produce relatively large strokes ($\approx 6 \mu\text{m}$) at modest applied potentials ($\approx 9 \text{ V}$).

Using Fractional Clock-Period Delays in Telemetry Arraying

Special digital FIR filters help to increase accuracy.

NASA's Jet Propulsion Laboratory, Pasadena, California

A set of special digital all-pass finite-impulse-response (FIR) filters produces phase shifts equivalent to delays that equal fractions of the sampling or clock period of a telemetry-data-processing system. These filters have been used to enhance the arraying of telemetry signals that have been received at multiple ground stations from spacecraft (see figure). Somewhat more specifically, these filters have been used to align, in the time domain, the telemetry-data sequences received by the various antennas, in order to maximize the signal-to-noise ratio of the composite telemetric signal obtained by summing the signals received by the antennas.

The term "arraying" in this context denotes a method of enhanced reception of telemetry signals in which several antennas are used to track a single spacecraft. Each antenna receives a signal that comprises a sum of telemetry data plus noise, and these sum data are sent to an arraying combiner for processing. Correlation is the means used to align the set of data from one antenna with that from another antenna. After the data from all the antennas have been aligned in the time do-

main, they are all added together, sample by sample. The desired result is (1) the coherent addition of the telemetry data to obtain an enhanced telemetry signal NS , where N is the number of antennas and S is an average telemetry signal received by one antenna; and (2) the addition of the uncorrelated noise components of the signals received by the various antennas to obtain a reduced (relative to the enhanced telemetry signal) noise signal of $N^{1/2}|V|$, where $|V|$ is a root-mean-square noise component of the signal received by an antenna.

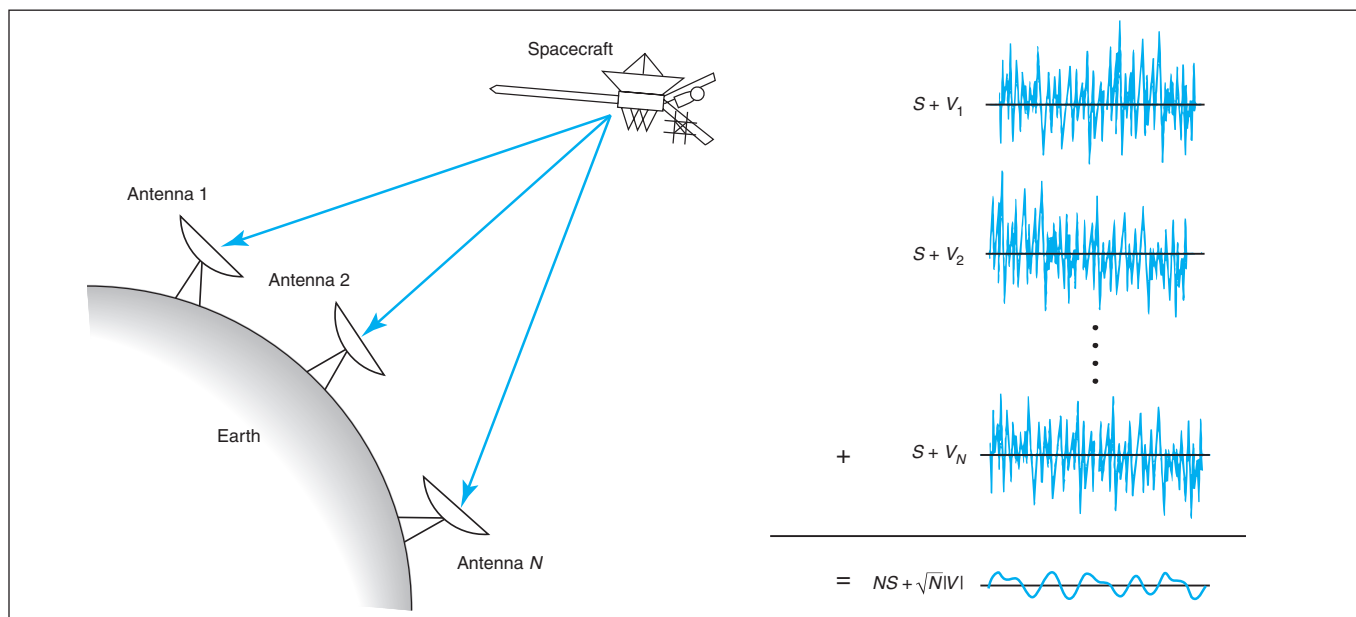
It must be emphasized that in order to obtain the desired result, one must align the timing of the data sequences from the various antennas as precisely as possible. This translates to a need to delay the various signals by various time intervals that could be as small as a fraction of a clock period.

One can construct special digital FIR filters that exhibit linear phase as long as their coefficients are symmetric around their centers. A filter of this type can be made to be of an all-pass type such that it produces group delay, based on the

length of the filter, equal to a whole number of clock periods if an odd number of coefficients are used. If an even number of coefficients are used, then the group delay can include half a clock period. By shifting the coefficients of such a filter to be slightly asymmetric, one can obtain a group delay that includes a fraction (not necessarily half) of a clock period.

This concept has been implemented through modification of the Parks-McLellan algorithm for generating equal-ripple FIR filters, in order to produce all pass filters with coefficients of varying asymmetry. This implementation has been found to yield filters that not only give the needed fractional-clock-period delays but also leave phases almost perfectly linear within the pass bands used for telemetry signals.

This work was done by Dr. David Fort, Dr. David Rogstad, and Stephen P. Rogstad of NASA's Jet Propulsion Laboratory. For further information, write to David Fort, Jet Propulsion Laboratory, 4800 Oak Grove Dr., Pasadena, CA 91109; call (818) 354-9132; or send electronic mail to david.n.fort@jpl.nasa.gov. NPO-21114



In **Spacecraft-Telemetry Arraying**, the telemetry signals plus noise received at multiple antennas are first aligned in time, then added to increase the signal-to-noise ratio.

▶ Developing Generic Software for Spacecraft Avionics

A standardized functional model would facilitate cost-effective reuse of common software modules.

NASA's Jet Propulsion Laboratory, Pasadena, California

A proposed approach to the development of software for spacecraft avionics is based partly on a concept of generic software that could be tailored to satisfy requirements for specific missions. The proposed approach would stand in contrast to the conventional approach of first defining avionics requirements for a specific mission, then developing software specific to those requirements. The proposed approach might also be adaptable to programming computers that control and monitor other complex equipment systems that range in scale from automobiles to factories.

The concept of a spacecraft avionics functional model (SAFM) is a major element of the proposed approach. An SAFM would be, essentially, a systematic and hierarchical description of the functionality required of the avionics software (and hardware) for a given mission. Although the initial input information used to start the construction of an SAFM would typically amount to a high-level description, the SAFM would thereafter be decomposed to a low level. The resulting low-level version of the model would be used to develop a set of generic requirements that could be expected to include a large fraction of all requirements for a large fraction of all missions. The generic requirements would be used to develop software modules that could be included in, or excluded from, the final flight software to satisfy the requirements of a specific mission.

By creating the opportunity to reuse common software modules on different missions, this approach would reduce the time, cost, and difficulty of developing the software. In addition, a high degree of reuse is expected to lead to increased reliability.

An SAFM would lend itself to any or all of the following five applications:

- *Education and Training*

The standard breakdown of functionality would be helpful in education and professional training in the functions that occur aboard a typical spacecraft.

- *Systems Engineering*

The breakdown would proceed, more specifically, from functions to subfunctions to roles. Such a breakdown would bring a standard template to part of the documentation of requirements. A standard template of this nature would increase the efficiency and enhance the utility of software tools used to document the requirements, while remaining flexible enough to be useful for a number of different projects. The standard template would, in effect, be a textual version of the hierarchy of the SAFM, placed into the functional-requirements portion of the requirements documentation for the spacecraft in question.

A key element of this approach is that at the breakdown-of-requirements stage of development of a given system, the requirements would be documented with respect to functionality but would not yet have been allocated to specific subsystems. It would still be possible, at this stage, to develop any of a number of different avionics architectures that would satisfy all the documented requirements.

- *Modeling of Resources*

The next step would be the estimation of the avionics resources used by each of the roles, and of how these avionics resources change with changes in the requirements of the roles. The next step would be to tabulate the resources required for each role, and then for each subfunction, in order to determine the resources used by each function. Once functions were assigned to subsystems, it would then be possible to determine the resources required by each subsystem.

- *Analysis, Tradeoffs, and Estimation of Costs*

If the modeling as described thus far were to be implemented with the help of an automated or semiautomated software tool, the next step would be to model a number of architectures and functional breakdowns. The architectures would differ in the functions assigned to

different hardware subsystems. This modeling would yield estimates of such parameters as memory usage, data and processor instruction rates, bus bandwidth, power usage, mass, and volume. These estimates could be used to determine which of the proposed architectures would best satisfy mission requirements, which would be most flexible, and how the different architectures would use system resources. The final step in modeling would be to estimate the costs of the candidate avionics architectures.

- *Functional Standardization and Commonality*

In an SAFM, the relationships among the roles within a subfunction would be the same. In other words, the roles would have constant functional contents, and their inputs and outputs would stay constant, or nearly so. This implies that if a role were used in more than one mission, it may be possible to reuse, from one spacecraft to another, the software module that implements that role. If this were done for a few missions, a library of software modules would soon be built up, making it possible for the next mission to limit itself to developing code for only those corresponding functional modules that were new, that were characterized by significantly different requirements, or that had grown antiquated.

This work was done by Joseph Smith of Caltech for NASA's Jet Propulsion Laboratory. Further information is contained in a TSP (see page 1).

In accordance with Public Law 96-517, the contractor has elected to retain title to this invention. Inquiries concerning rights for its commercial use should be addressed to

Intellectual Property group

JPL

Mail Stop 202-233

4800 Oak Grove Drive

Pasadena, CA 91109

(818) 354-2240

Refer to NPO-20968, volume and number of this NASA Tech Briefs issue, and the page number.



Numerical Study of Pyrolysis of Biomass in Fluidized Beds

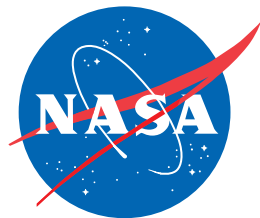
A report presents a numerical-simulation study of pyrolysis of biomass in fluidized-bed reactors, performed by use of the mathematical model described in “Model of Fluidized Bed Containing Reacting Solids and Gases” (NPO-30163), which appears elsewhere in this issue of *NASA Tech Briefs*. The purpose of the study was to investigate the effect of various operating conditions on the efficiency of production of condensable tar from biomass. The numerical results indicate that for a fixed particle size, the fluidizing-gas temperature is the foremost parameter that affects the tar yield. For the range of fluidizing-gas temperatures investigated, and under the assumption that the pyrolysis rate exceeds the feed rate, the optimum steady-state tar collection was found to occur at 750 K. In cases in which the assumption was not valid, the optimum temperature for tar collection was found to be only slightly higher. Scaling up of the reactor was found to exert a small negative effect on tar collection at the optimal operating temperature. It is also found that slightly better scaling is obtained by use of shallower fluidized beds with greater fluidization velocities.

*This work was done by Josette Bellan and Danny Lathouwers of Caltech for NASA’s Jet Propulsion Laboratory. Further information is contained in a TSP (see page 1).
NPO-30164*

Assessment of Models of Chemically Reacting Granular Flows

A report presents an assessment of a general mathematical model of dense, chemically reacting granular flows like those in fluidized beds used to pyrolyze biomass. The model incorporates submodels that have been described in several *NASA Tech Briefs* articles, including “Generalized Mathematical Model of Pyrolysis of Biomass” (NPO-20068) *NASA Tech Briefs*, Vol. 22, No. 2 (February 1998), page 60; “Model of Pyrolysis of Biomass in a Fluidized-Bed Reactor” (NPO-20708), *NASA Tech Briefs*, Vol. 25, No. 6 (June 2001), page 59; and “Model of Fluidized Bed Containing Reacting Solids and Gases” (NPO-30163), which appears elsewhere in this issue. The model was used to perform computational simulations in a test case of pyrolysis in a reactor containing sand and biomass (i.e., plant material) particles through which passes a flow of hot nitrogen. The boundary conditions and other parameters were selected for the test case to enable assessment of the validity of some assumptions incorporated into submodels of granular stresses, granular thermal conductivity, and heating of particles. The results of the simulation are interpreted as partly affirming the assumptions in some respects and indicating the need for refinements of the assumptions and the affected submodels in other respects.

*This work was done by Josette Bellan and Danny Lathouwers of Caltech for NASA’s Jet Propulsion Laboratory. Further information is contained in a TSP (see page 1).
NPO-30264*



National Aeronautics and
Space Administration